chemistry

MDPI

Article

Multicomponent Electrocatalytic Selective Approach to Unsymmetrical Spiro[furo[3,2-*c*]pyran-2,5′-pyrimidine] Scaffold under a Column Chromatography-Free Protocol at Room Temperature

Yuliya E. Ryzhkova [1,*], Michail N. Elinson [1], Anatoly N. Vereshchagin [1], Kirill A. Karpenko [1], Fedor V. Ryzhkov [1], Ivan E. Ushakov [2] and Mikhail P. Egorov [1]

[1] N.D. Zelinsky Institute of Organic Chemistry Russian Academy of Sciences, 47 Leninsky Prospekt, 119991 Moscow, Russia; elinson@ioc.ac.ru (M.N.E.); vereshchagin@ioc.ac.ru (A.N.V.); karpenkok_09@mail.ru (K.A.K.); ryzhkovfv@ioc.ac.ru (F.V.R.); mpe@ioc.ac.ru (M.P.E.)

[2] A.N. Nesmeyanov Institute of Organoelement Compounds Russian Academy of Sciences, 28 Vavilova St., 119991 Moscow, Russia; f0rbmen@gmail.com

* Correspondence: yu_ryzhkova@ioc.ac.ru

Abstract: Electrochemical synthesis suggested a mild, green and atom-efficient route to interesting and useful molecules, thus avoiding harsh chemical oxidizing and reducing agents used in traditional synthetic methods. Organic electrochemistry offers an excellent alternative to conventional methods of organic synthesis and creates a modern tool for carrying out organic synthesis, including cascade and multicomponent ones. In this research, a novel electrocatalytic multicomponent transformation was found: the electrochemical multicomponent assembly of arylaldehydes, *N*,*N*′-dimethylbarbituric acid and 4-hydroxy-6-methyl-2*H*-pyran-2-one in one pot reaction was carried out in alcohols in an undivided cell in the presence of alkali metal halides with the selective formation of substituted unsymmetrical 1′,3′,6-trimethyl-3-aryl-2′*H*,3*H*,4*H*-spiro[furo[3,2-*c*]pyran-2,5′-pyrimidine]-2′,4,4′,6′(1′*H*,3′*H*)-tetraones in 73–82% yields. This new electrocatalytic process is a selective, facile and efficient way to obtain spiro[furo[3,2-*c*]pyran-2,5′-pyrimidines]. According to screening molecular docking data using a self-made Python script in Flare, all synthesized compounds may be prominent for different medical applications, such as breast cancer, neurodegenerative diseases and treatments connected with urinary tract, bones and the cardiovascular system.

Keywords: electrolysis; electrocatalysis; multicomponent reaction; mediators; undivided cell; electrosynthesis; arylaldehydes; 4-hydroxy-6-methyl-2*H*-pyran-2-one; *N*,*N*′-dimethylbarbituric acid; spiro[furo[3,2-*c*]pyran-2,5′-pyrimidine]; docking studies

Citation: Ryzhkova, Y.E.; Elinson, M.N.; Vereshchagin, A.N.; Karpenko, K.A.; Ryzhkov, F.V.; Ushakov, I.E.; Egorov, M.P. Multicomponent Electrocatalytic Selective Approach to Unsymmetrical Spiro[furo[3,2-*c*]pyran-2,5′-pyrimidine] Scaffold under a Column Chromatography-Free Protocol at Room Temperature. *Chemistry* **2022**, *4*, 615–629. https://doi.org/10.3390/chemistry4020044

Academic Editor: Xiaodong Zhuang

Received: 31 May 2022
Accepted: 17 June 2022
Published: 19 June 2022

1. Introduction

The privileged structures or scaffolds have become the most efficient route in the search for pharmaceutical active compounds [1]. Merck researchers have introduced this definition in their study on benzodiazepines [2]. These scaffolds mainly are the rigid heterocyclic compounds, with special orientation of functional substituents for target recognition. The creation of a facile green and efficient method for selective synthesis of privileged scaffolds in the domino or multicomponent processes is now an important goal of modern organic chemistry [3,4].

A multicomponent strategy is now a route to achieve high efficiency and operation simplicity with simultaneous decreasing waste formation [5]. Multicomponent reactions (MCRs) are also characterized by a high bond-forming index (BFI) as several non-hydrogen atom bonds are formed in one-pot transformation [6]. The design of MCRs is a rapidly expanding area of research in the field of organic chemistry [7–9]. Thus, MCRs are now a useful strategy for the synthesis of complex heterocyclic structures.

Organic electrosynthesis has emerged in recent decades as a part of modern organic synthesis, which has set the stage for innovative chemical processes using novel mechanistic pathways [10–13]. Nevertheless, the use of electrochemical methods is still limited by equipment and procedure complexity, as well as long reaction time.

Thus, the most facile and efficient electrochemical strategy is the electrocatalytic transformation of organic compounds in the presence of mediators [14]. Among a variety of mediators, the halide anion/halogen pair is one of the most often used mediators for the selective and complex electro-organic transformations [15]. The use of alkali metal and ammonium halides as mediators has a number of advantages, such as inexpensive cost, environmental friendliness and in situ generation of molecular halogen.

C–H acids are useful reagents for the electrochemical processes with alkali metal halides as mediators in an undivided electrolyzer [16–20]. The electrocatalytic synthesis of substituted cyclopropanes and related spirocyclopropanes is a special and useful part of these electrocatalytic transformations [21–23]. Electrocatalytic reactions of heterocyclic C–H acids have also been intensively studied [24], as they afford the synthesis of different classes of heterocyclic compounds with a wide range of bioactivity [25].

The exploration of privileged structures or scaffolds in drug discovery is a rapidly emerging part of the medicinal chemistry [26]. Barbiturates (pyrimidine-2,4,6-triones) are known as privileged medicinal scaffold [27] in different central nervous system drugs, including sedatives, anticonvulsants, and anesthetics [28–30]. Nowadays, a renewed interest arose because it was found that the pyrimidinetrione template is an efficient zinc-chelating moiety [31], and thus, various pyrimidine-2,4,6-trione derivatives demonstrated high selectivity toward matrix metalloproteinases responsible for cancer progression. Additionally, barbiturates demonstrated inhibition against protein kinase C (PKC), an isoenzyme that is a target for therapeutic intervention of immunological disorders, human immunodeficiency virus and rheumatoid arthritis as well as inflammatory diseases [32].

2*H*-Pyran-2-one and its derivatives are also well-known in pharmacology. Derivatives of 4-hydroxy-2*H*-pyran-2-ones exhibit anti-HIV [33] and anticancer [34] properties. Among natural compounds containing 2*H*-pyran-2-one fragment, bufalin is a cardiotonic steroid and anti-cancer agent [35]. Other 2*H*-pyran-2-one derivatives have shown plant growth-regulating [36] antitumor [37] and HIV protease inhibiting activity [38].

Spirocycles have been employed as core structures and are widely used in drug discovery [39]. Owing to their inherent three-dimensionality and structural novelty, spiro scaffolds have been increasingly utilized in drug discovery [40]. Spirocycle compounds have a good balance between conformational rigidity and flexibility, which increase the chances of finding bioactive hits [41]. Barbiturate-incorporated spirocycles constitute a class of chemical entities with a wide range of biological activities and important medical applications [42]. Thus, spirobarbiturates have been established to exhibit neuropharmacological effects [43]. They are inhibitors of matrix metalloproteinase 13 (MMP-13) [44] and dihydroorotate dehydrogenase (DHODase) [45]. Recently, 1-phenyl-5,7-diazaspiro[2.5]octane-4,6,8-trione has been recognized as a tumor necrosis factor-alpha (TNF-α)-converting enzyme and matrix metalloproteinase inhibitor, and thus it could be utilized in the treatment of various inflammatory, infectious, immunological, or malignant diseases [46].

Taking into consideration our experience carrying out electrocatalytic cascade and multicomponent reactions with the formation of different types of spirocyclic compounds [47–51] and sufficient biomedical applications of spirocyclic barbiturates, we planned to design an efficient electrochemical multicomponent methodology for the direct conversion of arylaldehydes **1**, *N*,*N*′-dimethylbarbituric acid, and 4-hydroxy-6-methyl-2*H*-pyran-2-one in a one-pot reaction into earlier unknown unsymmetric substituted 3-aryl-2′*H*,3*H*,4*H*-spiro[furo[3,2-*c*]pyran-2,5′-pyrimidine]-2′,4,4′,6′(1′*H*,3′*H*)-tetrones **2**.

2. Materials and Methods

2.1. General Information

The solvents and reagents were purchased from commercial sources and used as received.

All melting points were measured with a Stuart SMP30 melting-point apparatus (Stuart Equipment, Cole-Parmer, UK) and were uncorrected. ^{1}H and ^{13}C-NMR spectra were recorded in $CDCl_3$ with Bruker AM300 spectrometer (Bruker Corporation, Billerica, MA, USA) at ambient temperature. Chemical shift values are relative to Me_4Si. The IR spectra were recorded with a Bruker ALPHA-T FT-IR spectrometer (Bruker Corporation, Billerica, MA, USA) in a KBr pellet. MS spectra (EI = 70 eV) were obtained directly with a Kratos MS-30 spectrometer (Kratos Analytical Ltd., Manchester, UK).

X-ray diffraction data were collected at 100K on a Bruker Quest D8 diffractometer (Bruker Corporation, Billerica, MA, USA) equipped with a Photon-III area-detector (graphite monochromator, shutterless φ- and ω-scan technique), using Mo Kα-radiation. The intensity data were integrated by the SAINT program [52] and corrected for absorption and decay using SADABS [53]. The structure was solved by direct methods using SHELXT [54] and refined on F [53] using SHELXL-2018 [55]. All non-hydrogen atoms were refined with anisotropic displacement parameters. Hydrogen atoms were placed in ideal calculated positions as riding atoms with relative isotropic displacement parameters; bond distances to H-atoms were refined. A rotating group model was applied for methyl groups. The SHELXTL program suite [52] was used for molecular graphics.

2.2. Electrocatalytic Multicomponent Synthesis of 1′,3′,6-Trimethyl-3-aryl-2′H,3H,4H-spiro-[furo[3,2-c]pyran-2,5′-pyrimidine]-2′,4,4′,6′(1′H,3′H)-tetraones **2a–i**

Arylaldehyde **1** (5 mmol), *N*,*N*′-dimethylbarbituric acid (5 mmol, 0.78 g), 4-hydroxy-6-methyl-2*H*-pyran-2-one (5 mmol, 0.63 g), and sodium iodide (3 mmol, 0.45 g), in methanol (20 mL) was electrolyzed in an undivided cell equipped with a magnetic stirrer, a graphite anode (5 cm^2) and an iron cathode (5 cm^2) at 20 °C under a constant current density 50 mA/cm^2 until the quantity of 2.8 F/mol of electricity was passed. After the electrolysis was finished, the reaction mixture was concentrated to a volume of 4 mL and cooled to 0 °C to crystallize the solid product, which was then filtered out, rinsed twice with an ice-cold ethanol/water solution (1:1, 4 mL) and dried under reduced pressure.

1′,3′,6-Trimethyl-3-phenyl-2′*H*,3*H*,4*H*-spiro[furo[3,2-*c*]pyran-2,5′-pyrimidine]-2′,4,4′,6′(1′*H*,3′*H*)-tetraone 2a, (white solid, 1.51 g, 82%), m.p. 249–251 °C (decomp.), FTIR (KBr) cm^{-1}: 3441, 3105, 2958, 2541, 1728, 1694, 1589, 1450, 1385, 1268, 1128, 1041. ^{1}H-NMR (300 MHz, $CDCl_3$) δ 2.38 (s, 3H, CH_3), 2.57 (s, 3H, CH_3), 3.43 (s, 3H, CH_3), 4.88 (s, 1H, CH), 6.28 (s, 1H, CH), 6.99–7.13 (m, 2H, 2 CH Ar), 7.30–7.40 (m, 3H, 3 CH Ar) ppm. ^{13}C-NMR (75 MHz, $CDCl_3$) δ 20.7, 28.3, 29,4, 58.9, 91.1, 95.5, 98.5, 128.4 (2C), 128.9 (2C), 129.4, 132.4, 149.8, 159.8, 163.5, 166.2, 167.8, 172.5 ppm. MS (EI, 70 eV) *m*/*z* (%): 368 $[M]^+$ (7), 325 (100), 268 (5), 240 (2), 199 (4), 156 (1), 155 (2), 127 (8), 102 (4), 43 (21). Anal. calcd. for $C_{19}H_{16}N_2O_6$: C, 61.96; H, 4.38; N, 7.61%. Found: C, 61.84; H, 4.33; N, 7.54%.

Crystal Data for **2a** (M = 368.34 g/mol): monoclinic, space group P21/c (No. 14), a = 7.7339 (4) Å, b = 18.4269 (11) Å, c = 12.0713 (7) Å, β = 97.8430 (10)°, V = 1704.21 (17) Å3, Z = 4, T = 120 °K, μ (MoKα) = 0.109 mm^{-1}, Dcalc = 1.436 g/cm^3, 23,459 reflections measured (4.06° ≤ 2Θ ≤ 61.202°), 5239 unique (R_{int} = 0.0553, R_{sigma} = 0.0464), which were used in all calculations. The final R_1 was 0.0455 (I > 2σ(I)) and wR_2 was 0.1146 (all data). CCDC 2,152,149 contains the supplementary crystallographic data for this paper. These data can be obtained free of charge from The Cambridge Crystallographic Data Centre via http://www.ccdc.cam.ac.uk (accessed on 1 March 2022).

3-(4-Methyl)-1′,3′,6-trimethyl-2′*H*,3*H*,4*H*-spiro[furo[3,2-*c*]pyran-2,5′-pyrimidine]-2′,4,4′,6′(1′*H*,3′*H*)-tetraone 2b, (white solid, 1.53 g, 80%), m.p. 290–291 °C (decomp.), FTIR (KBr) cm^{-1}: 3448, 3099, 2926, 2526, 1739, 1643, 1587, 1380, 1108. ^{1}H-NMR (300 MHz, $CDCl_3$) δ 2.33 (s, 3H, CH_3), 2.37 (s, 3H, CH_3), 2.60 (s, 3H, CH_3), 3.43 (s, 3H, CH_3), 4.85 (s, 1H, CH), 6.27 (s, 1H, CH), 6.93 (d, ^{3}J = 8.2 Hz, 2H, 2 CH Ar), 7.14 (d, ^{3}J = 8.2 Hz, 2H, 2 CH Ar) ppm. ^{13}C-NMR (75 MHz, $CDCl_3$) δ 20.7, 21.2, 28.4, 29.5, 58.8, 91.2, 95.5, 98.7, 128.3 (2C), 129.3 (2C), 129.7, 139.5, 149.9, 159.8, 163.7, 166.3, 167.7, 172.4 ppm. MS (EI, 70 eV) *m*/*z* (%): 382

$[M]^+$ (3), 339 (100), 282 (7), 267 (2), 169 (5), 156 (11), 141 (8), 115 (17), 85 (7). Anal. calcd. for $C_{20}H_{18}N_2O_6$: C, 62.82; H, 4.75; N, 7.33%. Found: C, 62.75; H, 4.66; N, 7.21%.

3-(3-Fluorophenyl)-1′,3′,6-trimethyl-2′*H*,3*H*,4H-spiro[furo[3,2-*c*]pyran-2,5′-pyrimidine]-2′,4,4′,6′(1′*H*,3′*H*)-tetraone 2c, (white solid, 1.45 g, 75%), m.p. 247–249 °C (decomp.), FTIR (KBr) cm^{-1}: 3434, 3091, 2958, 2388, 1690, 1590, 1447, 1264, 1036. ^{1}H-NMR (300 MHz, $CDCl_3$) δ 2.39 (s, 3H, CH_3), 2.67 (s, 3H, CH_3), 3.44 (s, 3H, CH_3), 4.86 (s, 1H, CH), 6.29 (s, 1H, CH), 6.71 (d, $^3J_{H\text{-}F}$ = 11.7 Hz, 1H, 1 CH Ar), 6.81–6.90 (m, 2H, 2 CH Ar), 7.19 (dd, $^3J_{H\text{-}F}$ = 14.4 Hz, $^3J_{H\text{-}H}$ = 6.5 Hz, 1H, 1 CH Ar) ppm. ^{13}C-NMR (75 MHz, $CDCl_3$) δ 20.7, 28.5, 29.5, 58.1, 90.8, 95.5, 98.3, 115.6 (d, $^2J_{C\text{-}F}$ = 22.2 Hz), 116.5 (d, $^2J_{C\text{-}F}$ = 22.2 Hz), 124.3 (d, $^4J_{C\text{-}F}$ = 2.8 Hz), 130.5 (d, $^3J_{C\text{-}F}$ = 7.6 Hz), 135.1 (d, $^3J_{C\text{-}F}$ = 7.6 Hz), 149.7, 159.7, 162.9 (d, $^1J_{C\text{-}F}$ = 248.2 Hz), 163.3, 165.9, 168.1, 172.7 ppm. MS (EI, 70 eV) *m*/*z* (%): 386 $[M]^+$ (3), 344 (19), 343 (100), 286 (5), 217 (5), 189 (2), 160 (8), 145 (6), 132 (2), 125 (4). Anal. calcd. for $C_{19}H_{15}FN_2O_6$: C, 59.07; H, 3.91; F, 4.92; N, 7.25%. Found: C, 58.98; H, 3.87; F, 4.85; N, 7.19%.

3-(4-Chlorophenyl)-1′,3′,6-trimethyl-2′*H*,3*H*,4*H*-spiro[furo[3,2-*c*]pyran-2,5′-pyrimidine]-2′,4,4′,6′(1′*H*,3′*H*)-tetraone 2d, (white solid, 1.57 g, 78%), m.p. 258–260 °C (decomp.), FTIR (KBr) cm^{-1}: 3435, 3098, 2962, 2361, 1720, 1686, 1587, 1445, 1380, 1044. ^{1}H-NMR (300 MHz, $CDCl_3$) δ 2.38 (s, 3H, CH_3), 2.67 (s, 3H, CH_3), 3.43 (s, 3H, CH_3), 4.85 (s, 1H, CH), 6.28 (s, 1H, CH), 6.99 (d, ^3J = 8.4 Hz, 2H, 2 CH Ar), 7.32 (d, ^3J = 8.4 Hz, 2H, 2 CH Ar) ppm. ^{13}C-NMR (75 MHz, $CDCl_3$) δ 20.7, 28.5, 29,6, 58.1, 90.8, 95.5, 98.3, 129.2 (2C), 129.9 (2C), 131.1, 135.6, 149.7, 159.7, 163.4, 166.0, 168.1, 172.6 ppm. MS (EI, 70 eV) *m*/*z* (%): 404 $[M]^+$ Cl^{37} (1), 402 $[M]^+$ Cl^{35} (3), 361 (34), 359 (100), 302 (3), 290 (3), 176 (8), 161 (4), 126 (7), 85 (11). Anal. calcd. for $C_{19}H_{15}ClN_2O_6$: C, 56.66; H, 3.75; Cl, 8.80; N, 6.96%. Found: C, 56.58; H, 3.71; Cl, 8.73; N, 6.85%.

1′,3′,6-Trimethyl-3-(4-nitrophenyl)-2′*H*,3*H*,4*H*-spiro[furo[3,2-*c*]pyran-2,5′-pyrimidine]-2′,4,4′,6′(1′*H*,3′*H*)-tetraone 2e, (white solid, 1.67 g, 81%), m.p. 262–264 °C (decomp.), FTIR (KBr) cm^{-1}: 3435, 3090, 2963, 1732, 1696, 1590, 1522, 1441, 1352, 1173, 1029. ^{1}H-NMR (300 MHz, $CDCl_3$) δ 2.41 (s, 3H, CH_3), 2.67 (s, 3H, CH_3), 3.46 (s, 3H, CH_3), 4.96 (s, 1H, CH), 6.31 (s, 1H, CH), 7.26 (d, ^3J = 8.5 Hz, 2H, 2 CH Ar), 8.21 (d, ^3J = 8.5 Hz, 2H, 2 CH Ar) ppm. ^{13}C-NMR (75 MHz, $CDCl_3$) δ 20.8, 28.5, 29,7, 57.7, 90.3, 95.5, 98.1, 124.0 (2C), 129.8 (2C), 139.8, 148.4, 149.5, 159.6, 163.0, 165.6, 168.6, 172.9 ppm. MS (EI, 70 eV) *m*/*z* (%): 413 $[M]^+$ (2), 372 (3), 371 (20), 370 (100), 325 (3), 324 (7), 323 (7), 244 (5), 187 (13), 156 (1), 141 (3), 126 (6), 85 (9). Anal. calcd. for $C_{19}H_{15}N_3O_8$: C, 55.21; H, 3.66; N, 10.17%. Found: C, 55.14; H, 3.59; N, 10.08%.

Methyl 4-(1′,3′,6-trimethyl-2′,4,4′,6′-tetraoxo-1′,3′,4′,6′-tetrahydro-2′*H*,3*H*,4*H*-spiro[furo pyran-2,5′-pyrimidin]-3-yl)benzoate 2f, (white solid, 1.64 g, 77%), m.p. 275–276 °C (decomp.), FTIR (KBr) cm^{-1}: 3435, 3100, 2954, 2846, 2391, 1724, 1592, 1440, 1283, 1113, 1036. ^{1}H-NMR (300 MHz, $CDCl_3$) δ 2.39 (s, 3H, CH_3), 2.39 (s, 3H, CH_3), 2.60 (s, 3H, CH_3), 3.45 (s, 3H, CH_3), 3.93 (s, 3H, CO_2Me), 4.92 (s, 1H, CH), 6.30 (s, 1H, CH), 7.14 (d, ^3J = 8.4 Hz, 2H, 2 CH Ar), 8.01 (d, ^3J = 8.4 Hz, 2H, 2 CH Ar) ppm. ^{13}C-NMR (75 MHz, $CDCl_3$) δ 20.7, 28.4, 29.5, 52.3, 58.3, 90.7, 95.5, 98.3, 128.7 (2C), 130.1 (2C), 131.1, 137.5, 149.7, 159.7, 163.3, 165.9, 166.2, 168.1, 172.7 ppm. MS (EI, 70 eV) *m*/*z* (%): 426 $[M]^+$ (2), 395 (3), 385 (3), 384 (22), 383 (100), 324 (9), 283 (3), 257 (4), 200 (10), 156 (2), 141 (4), 126 (5), 85 (8), 43 (22). Anal. calcd. for $C_{21}H_{18}N_2O_8$: C, 59.16; H, 4.26; N, 6.57%. Found: C, 59.08; H, 4.21; N, 6.45%.

1′,3′,6-Trimethyl-3-(pyridin-3-yl)-2′*H*,3*H*,4*H*-spiro[furo[3,2-*c*]pyran-2,5′-pyrimidine]-2′,4,4′,6′(1′*H*,3′*H*)-tetraone 2g, (white solid, 1.35 g, 73%), m.p. 236–240 °C (decomp.), FTIR (KBr) cm^{-1}: 3434, 3090, 2957, 1741, 1685, 1583, 1448, 1281, 1040. ^{1}H-NMR (300 MHz, $CDCl_3$) δ 2.39 (s, 3H, CH_3), 2.68 (s, 3H, CH_3), 3.45 (s, 3H, CH_3), 4.90 (s, 1H, CH), 6.30 (s, 1H, CH), 7.30 (d, ^3J = 5.1 Hz 1H, 1 CH Ar), 7.40 (dt, ^3J = 7.7 Hz, ^4J = 2.1 Hz, 1H, 1 CH Ar), 8.34 (d, ^4J = 2.1 Hz 1H, 1 CH Ar), 8.61 (dd, ^3J = 4.6 Hz, ^2J = 2.1 Hz, 1H, 1 CH Ar) ppm. ^{13}C-NMR (75 MHz, $CDCl_3$) δ 20.8, 28.6, 29,7, 56.2, 90.5, 95.5, 97.8, 123.7 (2C), 128.8, 136.2 (2C), 149.7 (2C), 150.8, 163.3, 165.8, 172.9 ppm. MS (EI, 70 eV) *m*/*z* (%): 369 $[M]^+$ (6), 327 (19), 326 (100),

269 (9), 172 (3), 156 (3), 143 (15), 129 (4), 115 (5), 69 (9), 43 (31). Anal. calcd. for $C_{18}H_{15}N_3O_6$: C, 58.54; H, 4.09; N, 11.38%. Found: C, 58.41; H, 4.03; N, 11.26%.

1′,3′,6-Trimethyl-3-(pyridin-4-yl)-2′*H*,3*H*,4*H*-spiro[furo[3,2-*c*]pyran-2,5′-pyrimidine]-2′,4,4′,6′(1′*H*,3′*H*)-tetraone 2h, (yellowish solid, 1.39 g, 75%), m.p. 190–192 °C (decomp.), FTIR (KBr) cm^{-1}: 3434, 3102, 2960, 1719, 1684, 1584, 1446, 1382, 1289, 1043. ^{1}H-NMR (300 MHz, $CDCl_3$) δ 2.39 (s, 3H, CH_3), 2.64 (s, 3H, CH_3), 3.43 (s, 3H, CH_3), 4.83 (s, 1H, CH), 6.29 (s, 1H, CH), 6.99 (d, ^3J = 6.1 Hz, 2H, 2 CH Ar), 8.59 (d, ^3J = 6.1 Hz, 2H, 2 CH Ar) ppm. ^{13}C-NMR (75 MHz, $CDCl_3$) δ 20.8, 28.4, 29,6, 57.5, 90.4, 95.5, 97.6, 123.4 (2C), 141.7, 149.6, 150.4 (2C), 159.5, 163.0, 165.7, 168.5, 173.1 ppm. MS (EI, 70 eV) m/z (%): 369 $[M]^+$ (3), 327 (20), 326 (100), 269 (8), 200 (7), 172 (3), 156 (4), 143 (18), 129 (4), 115 (4), 69 (14), 43 (38). Anal. calcd. for $C_{18}H_{15}N_3O_6$: C, 58.54; H, 4.09; N, 11.38%. Found: C, 58.50; H, 4.05; N, 11.31%.

1′,3′,6-Trimethyl-3-(naphthalen-1-yl)-2′*H*,3*H*,4*H*-spiro[furo[3,2-*c*]pyran-2,5′-pyrimidine]-2′,4,4′,6′(1′*H*,3′*H*)-tetraone 2i, (yellowish solid, 1.63 g, 78%), m.p. 255–257 °C (decomp.), FTIR (KBr) cm^{-1}: 3436, 3271, 2957, 2658, 2351, 1732, 1588, 1448, 1379, 1127, 1034. ^{1}H-NMR (300 MHz, $CDCl_3$) δ 2.15 (s, 3H, CH_3), 2.41 (s, 3H, CH_3), 3.35 (s, 3H, CH_3), 5.93 (s, 1H, CH), 6.32 (s, 1H, CH), 7.26–7.31 (m, 1H, 1 CH Ar), 7.43–7.57 (m, 3H, 3 CH Ar), 7.65–7.72 (m, 1H, 1 CH Ar), 7.82–7.94 (m, 2H, 2 CH Ar) ppm. ^{13}C-NMR (75 MHz, DMSO-d_6) δ 20.7, 28.0, 29,3, 53.7, 90.7, 95.6, 98.9, 121.0, 125.5, 126.1, 126.9, 127.5, 127.8, 129.6, 129.7, 131.4, 133.9, 149.1, 159.8, 163.7, 166.3, 167.8, 172.8 ppm. MS (EI, 70 eV) m/z (%): 418 $[M]^+$ (73), 377 (3), 376 (26), 375 (100), 303 (14), 302 (10), 261 (13), 234 (9), 177 (30), 176 (40), 156 (1), 127 (14), 43 (85). Anal. calcd. for $C_{23}H_{18}N_2O_6$: C, 66.03; H, 4.34; N, 6.70%. Found: C, 65.94; H, 4.30; N, 6.63%.

3. Results and Discussion

3.1. Electrocatalytic Multicomponent One-Pot Synthesis of Spiro[furo[3,2-b]pyran-2,5′-pyrimidines] **2a–i**

In our research, we report the results on the multicomponent electrochemical one-pot assembly of arylaldehydes **1a–i**, *N*,*N*′-dimethylbarbituric acid and 4-hydroxy-6-methyl-2*H*-pyran-2-one into unsymmetrical substituted 3-aryl-2′*H*,3*H*,4*H*-spiro[furo[3,2-*c*]pyran-2,5′-pyrimidine]-2′,4,4′,6′(1′*H*,3′*H*)-tetrones **2a–i** in alcohols in an undivided electrolyzer in the presence of alkali halides as mediators (Schemes 1 and 2, Tables 1 and 2).

During the first step of our study, to estimate the synthetic potential of the electrochemical method and to carefully estimate the electrolytic conditions, the electrolysis of benzaldehyde **1a**, *N*,*N*′-dimethylbarbituric acid, and 4-hydroxy-6-methyl-2*H*-pyran-2-one in alcohols as solvent in an undivided cell in the presence of alkali halides as mediators was specially studied (Scheme 2, Table 1).

At the beginning of this research, methanol was used as solvent and lithium bromide as the mediator. Under this electrolysis condition in an undivided electrolyzer after 2 F/mol of electricity were passed, spiro[furo[3,2-*b*]pyran-2,5′-pyrimidine] **2a** was obtained in 48% yields (Entry 1, Table 1). Similar results, 52 and 50% yields of **2a,** were found using sodium and potassium bromides as mediators (Entries 2 and 3, Table 1). Among iodides as mediators (Entries 4–7, Table 1), the best result was in the case of sodium iodide as mediator with 59% yield of spiro[furo[3,2-*b*]pyran-2,5′-pyrimidine] **2a**. Other alcohols-ethanol and *n*-propanol were found less suitable in this electrochemical multicomponent process (Entries 8 and 9, Table 1). The next improvement was achieved with an increasing quantity of electricity passed through the undivided cell (Entries 10–14, Table 1). When 2.8 F/mol of electricity was used, spiro[furo[3,2-*b*]pyran-2,5′-pyrimidine] **2a** was obtained in best 82% yield.

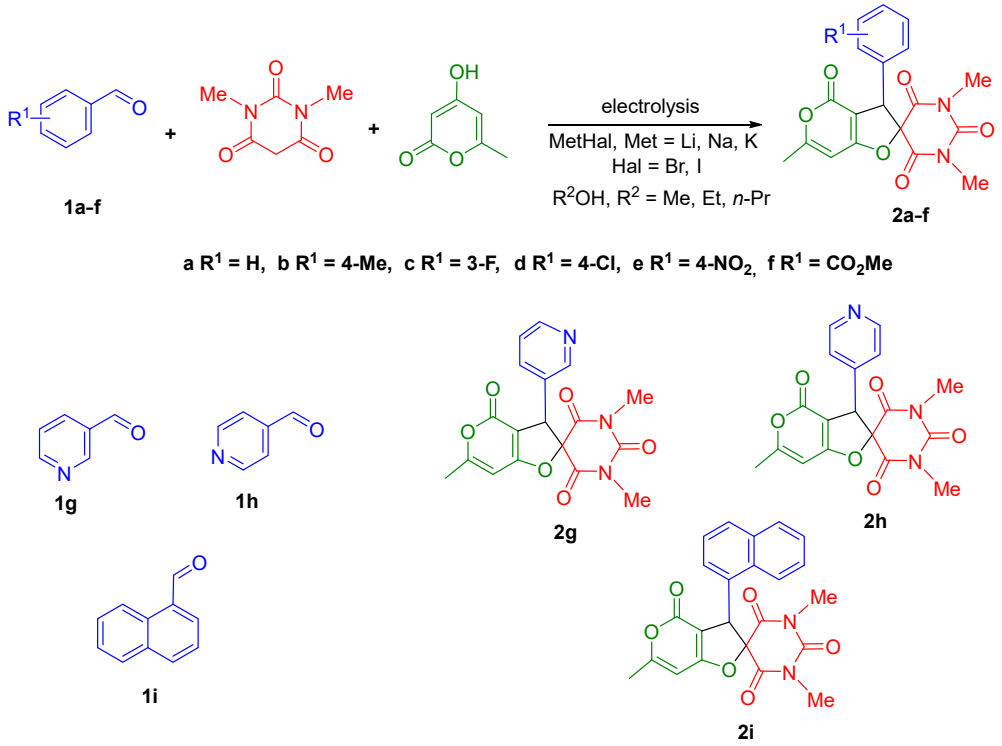

Scheme 1. Electrocatalytic multicomponent one-pot synthesis of spiro[furo[3,2-*b*]-pyran-2,5′-pyrimidines] **2a**–**i**.

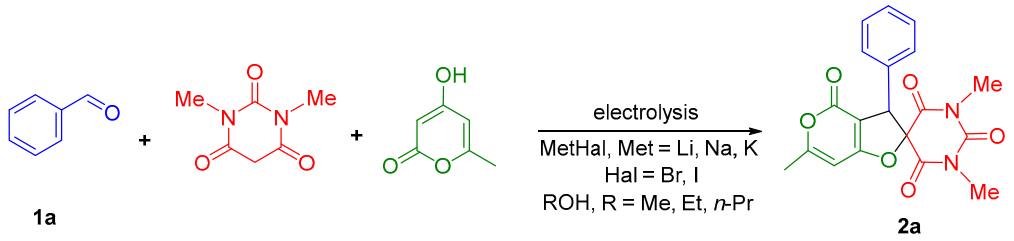

Scheme 2. Electrocatalytic multicomponent one-pot synthesis of spiro[furo[3,2-*b*]-pyran-2,5′-pyrimidines] **2a**–**i**.

Table 1. Electrocatalytic multicomponent synthesis of spiro[furo[3,2-*b*]pyran-2,5′-pyrimidine] **2a**.

Entry	Solvent	Mediator	Time/min	Electricity F/mol	Yield of 2a (%)
1	MeOH	LiBr	64	2.0	48
2	MeOH	NaBr	64	2.0	52
3	MeOH	KBr	64	2.0	50
4	MeOH	LiI	64	2.0	54
5	MeOH	NaI	64	2.0	59
6	MeOH	KI	64	2.0	57
7	MeOH	NH_4I	64	2.0	43
8	EtOH	NaI	64	2.0	52
9	*n*-PrOH	NaI	64	2.0	48
10	MeOH	NaI	70	2.2	63
11	MeOH	NaI	77	2.4	67
12	MeOH	NaI	83	2.6	70
13	MeOH	NaI	90	2.8	82
14	MeOH	NaI	96	3.0	71

Electrolysis conditions: Benzaldehyde **1a** (5 mmol), *N*,*N*′-dimethylbarbituric acid (5 mmol), 4-hydroxy-6-methyl-2*H*-pyran-2-one (5 mmol), mediator (3 mmol), alcohol (20 mL), iron cathode (5 cm^2), graphite anode (5 cm^2), undivided cell, constant current density 50 mA/cm^2, 20 °C.

Table 2. Electrocatalytic multicomponent synthesis of spiro[furo[3,2-*b*]pyran-2,5′-pyrimidine] **2a–i**.

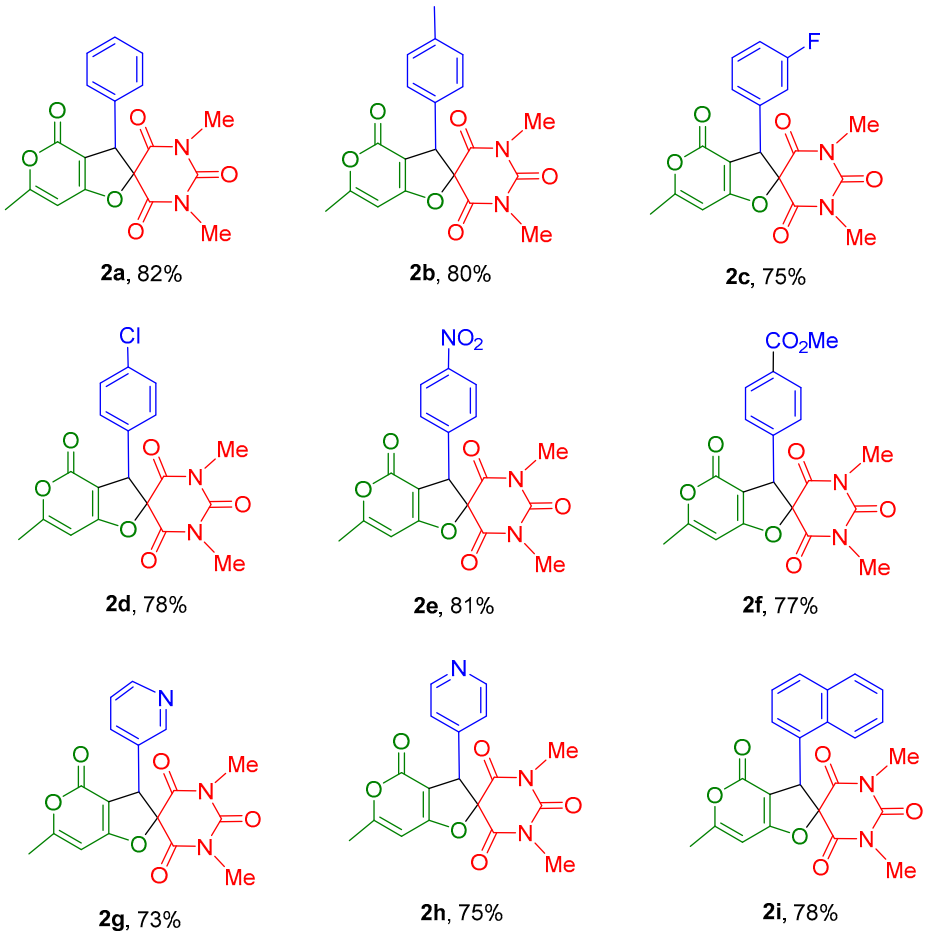

Electrolysis conditions: Arylaldehydes **1a–i** (5 mmol), *N*,*N*′-dimethylbarbituric acid (5 mmol), 4-hydroxy-6-methyl-2*H*-pyran-2-one (5 mmol), NaI (3 mmol), MeOH (20 mL), iron cathode (5 cm^2), graphite anode (5 cm^2), undivided cell, constant current density 50 mA/cm^2, 2.8 F/mol electricity passed (90 min) at 20 °C.

Under these optimal conditions, unsymmetrical spiro[furo[3,2-*b*]pyran-2,5′-pyrimidines] **2a–i** were obtained in 73–82% yields in a one-pot electrocatalytic reaction from aldehydes **1a–i**, *N*,*N*′-dimethylbarbituric acid and 4-hydroxy-6-methyl-2*H*-pyran-2-one (Table 2).

When the electrochemical process was finished, the reaction mixture was concentrated by evaporation *in vacuo* on a rotary evaporator to a volume of 4 mL and chilled to 0 °C. Under these conditions, a solid precipitate formed, which was then filtered out, treated twice with a cold ethanol/water solution (1:1 *v*/*v*, 4 mL) and dried under reduced pressure.

The structures of spirobarbituric dihydrofurans **2a–i** were proven by ^{1}H, ^{13}C NMR, IR spectroscopy, mass spectrometry data and elemental analysis. For all compounds, only one set of signals was observed in ^{1}H and ^{13}C NMR spectra.

Structure spiro[furo[3,2-*b*]pyran-2,5′-pyrimidine] **2a** was additionally confirmed by an X-ray diffraction study (see Supplementary Materials and Figure 1).

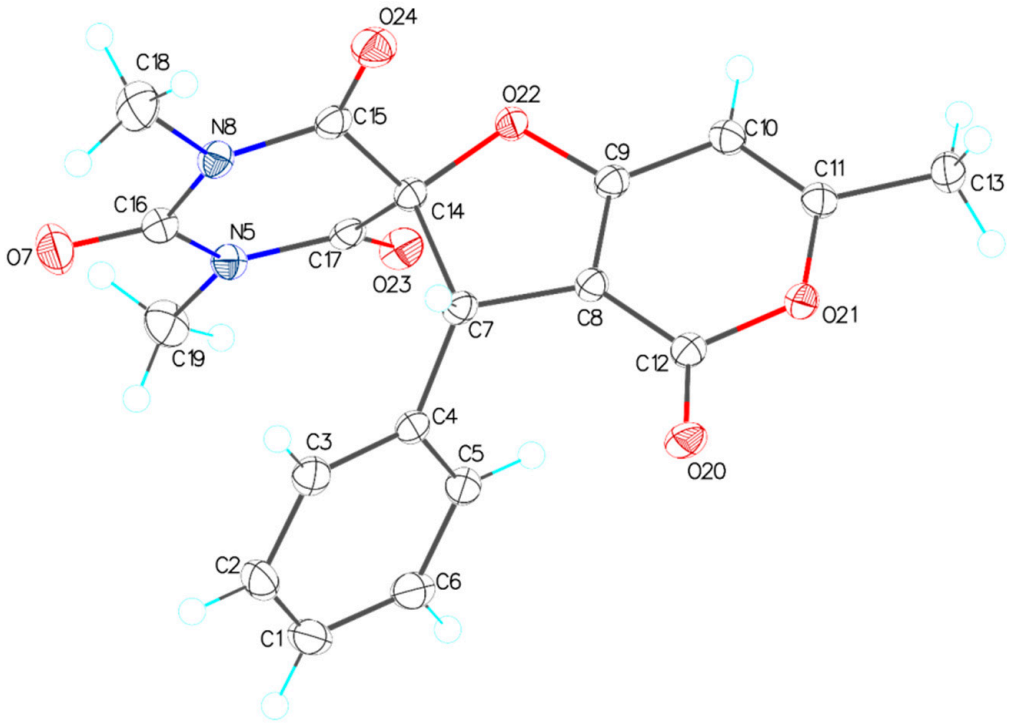

Figure 1. The general view of compound **2a** in crystal. Atoms are represented by thermal displacement ellipsoids (p = 50%).

With all above results and taking into consideration the data on electrocatalytic reactions mediated by iodides [56–58], the following mechanism for the electrocatalyic multicomponent transformation of benzaldehyde **1a,** *N*,*N*′-dimethylbarbituric acid and 4-hydroxy-6-methyl-2*H*-pyran-2-one into unsymmetrical spiro[furo[3,2-*b*]-pyran-2,5′-pyrimidine] **2a** was suggested (Scheme 3).

The formation of hydrogen is the cathodic process. During this process, a methoxide anion is also formed. The generation of iodine is an anodic process and the iodine color was observed at the anode, if the stirring of the reaction mixture is stopped.

Reaction in a solution medium between a methoxide ion and *N*,*N*′-dimethylbarbituric acid leads to the anion of *N*,*N*′-dimethylbarbituric acid **A** formation (Scheme 3). Then, Knoevenagel condensation of benzaldehyde **1a** with *N*,*N*′-dimethylbarbituric acid anion **A** results in Knoevenagel adduct **3** formation with the elimination of a hydroxide anion. The following hydroxide anion induced Michael addition of 4-hydroxy-6-methyl-2*H*-pyran-2-one to the electron-deficient Knoevenagel adduct **3** leads to the formation of corresponding anion **B**. The subsequent iodination of anion **B** by generated-at-anode iodine, affords 5-iodo-5-[(4-hydroxy-6-methyl-2-oxo-2*H*-pyran-3-yl)(phenyl)methyl]-1,3-dimethylpyrimidine-2,4,6(1*H*,3*H*,5*H*)-trione **4**, which in the next step is cyclized by the action of the second methoxide anion into the unsymmetrical spiro[furo[3,2-*b*]pyran-2,5′-pyrimidine] **2a** with the regeneration of the bromide ion.

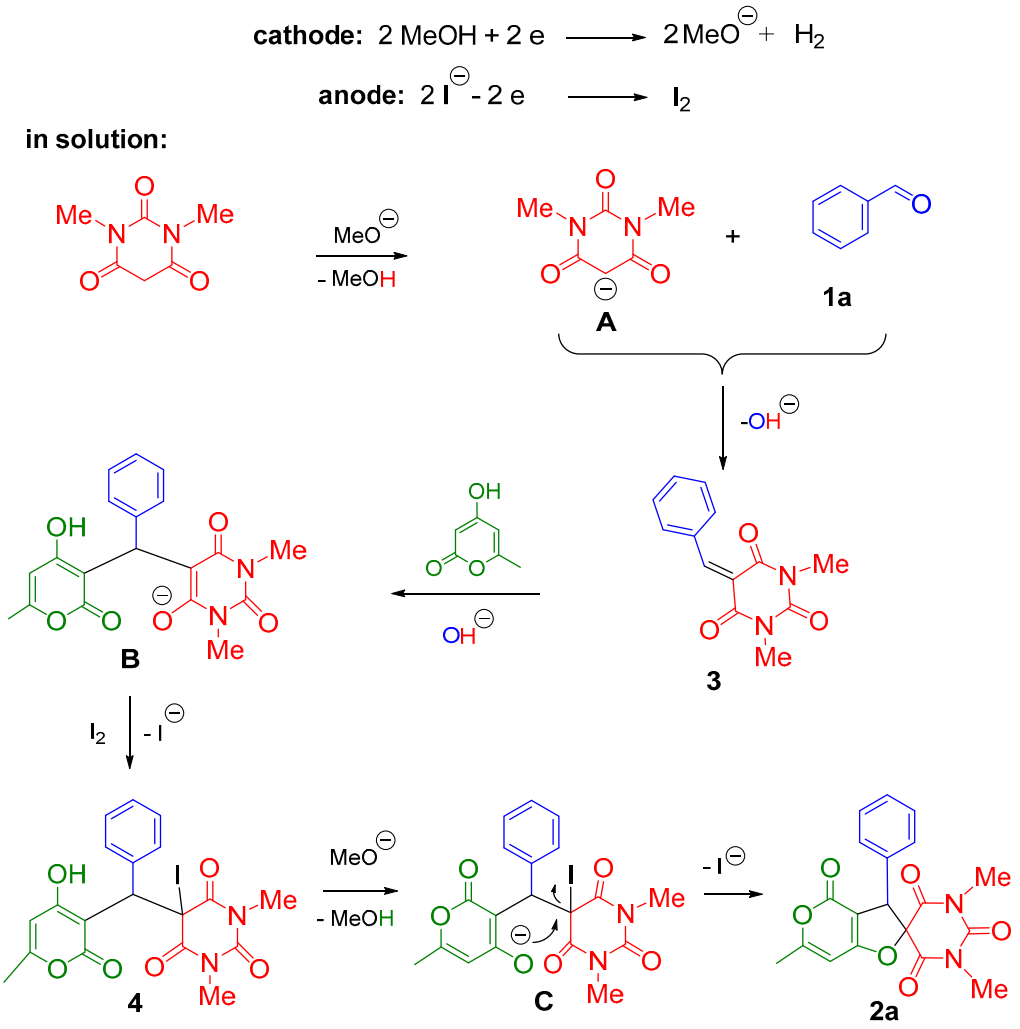

Scheme 3. The mechanism of electrocatalytic multicomponent one-pot synthesis of spiro[furo[3,2-*c*]pyran-2,5′-pyrimidine] **2a**.

3.2. Docking Study

To propose a potential application of synthesized compounds, they were subjected to docking procedure. Then, 169 Entries from rcsb.org were selected for the procedure and synthesized compounds were docked into them. To embrace all the proposed proteins, the docking procedure was performed in automated regime using self-made Python script (see information in Appendix A). Utilization of Python scripts for docking is available in Flare, which was used for this study [59–63].

PDB structures of each target were automatically downloaded from the PDB-bank (rcsb.org). To download all entries, the python script "downloader.py" was used. This script handles each PDB entry from the text file in the same directory, and then downloads the appropriate PDB structure.

The downloaded PDB structures were prepared for the docking procedure. This included capping chains, extracting ligand and removing waters outside the active site (out of range of 6A). To handle that, the python script "proteinprep.py" (available as a Flare extension) was used. The synthesized compounds (ligands) were subjected to a docking procedure into prepared PDB structures. The docking was performed in "Exhaustive" mode. To automate this procedure, the python-script "docking.py" (available Flare as extension) was used.

As long as this routine was demanded for each protein–ligand pair, the whole computation (all 169 PDB-entries) was performed using python script "script.py". This subprogram

sequentially calls commands of protein preparation, extraction of reference ligand, docking of synthesized ligands and outputs the results into separate text files. It utilizes the scripts described above ("proteinprep.py", "docking.py"). The output from the docking procedure (text files) was converted into an Excel table by another script ("outpt_prep.py"). The result is presented in Table 3. The average energies of protein–ligand interactions were calculated (in Excel file, see archive attached to the article) to define the most prominent target to the whole synthesized class of ligands. The results of the docking procedure are shown in Table 3.

Table 3. The energy of interaction of 13 predicted protein–ligand pairs in kcal/mol (10 was the most favorable and 3 was the least favorable). The results for other 156 structures could be found in supporting information. PDB entries obtained from rcsb.org.

Structure	2a	2b	2c	2d	2e	2f	2g	2h	2i	AVG
1m9m	–8.7	–9.5	–8.9	–9.2	–8.5	–9.1	–8.0	–7.9	–9.1	–8.8
2xas	–8.4	–9.3	–8.9	–10.0	–8.6	–10.4	–8.1	–7.9	–9.2	–9.0
4iw8	–9.0	–9.5	–9.2	–9.6	–8.6	–9.7	–8.4	–8.6	–10.0	**–9.2**
4p6x	–8.7	–9.0	–9.0	–10.1	–8.4	–8.8	–8.4	–8.3	–8.7	–8.8
5tlt	–8.8	–9.3	–8.7	–9.5	–8.8	–9.4	–8.5	–8.4	–10.0	**–9.0**
5vv1	–8.9	–9.3	–9.1	–9.4	–8.5	–9.6	–7.3	–7.2	–9.5	–8.8
6kbp	–9.8	–9.3	–9.9	–10.2	–8.3	–9.8	–7.1	–8.0	–9.2	**–9.1**
6nh5	–8.7	–9.3	–8.8	–9.4	–8.5	–9.3	–7.8	–7.7	–9.4	–8.8
6nhb	–9.1	–9.6	–9.2	–9.6	–8.2	–9.1	–7.8	–7.7	–9.5	–8.9
6ud5	–8.7	–9.2	–8.6	–9.5	–8.8	–9.5	–7.9	–8.2	–9.5	–8.9
2axa	–6.3	–4.9	–4.8	–5.2	–4.1	–3.8	–4.9	–4.9	–4.9	–4.9
3vng	–5.9	–5.4	–5.6	–7.0	–6.4	–5.5	–4.6	–5.7	–6.2	–5.8
5i6x	–4.3	–4.8	–4.6	–4.7	–4.9	–4.7	–4.4	–4.4	–4.6	–4.6

The calculation of docking modes was accomplished for 146 proteins from all 169 proposed entries. The docking procedure was interrupted for 23 proteins because of program termination (the list of proteins for calculation that were not accomplished can be found in the supporting information).

For the proposed proteins, the most favorable interactions were given by *para*-chloro substituted compound **2d**. The average energy of protein–ligand interaction for **2d** with proposed proteins is close to −9.7 kcal/mol. According to docking results, carbomethoxy substituted **2f** (*para*-substituent) and 1-naphthyl substituted **2i** were slightly less active, the energies of protein–ligand interaction were close to −9.5 and −9.4 kcal/mol on average.

At the same time, among calculated protein–ligand interactions the most favorable result was given by 4iw8 [64], the average interaction energy of substituted compounds with this structure is of −9.2 kcal/mol. There is also 5tlt structure [65] with the average binding energy of −9.0 kcal/mol. Both 4iw8 and 5tlt are proteins, estrogen receptor α subtype, with modulators (removed during the docking procedure). The estrogen receptor α is an effective target in breast cancer therapies [66], It is distributed among reproductive, central nervous, skeletal, and cardiovascular systems and has important actions in the urinary tract, mucous, skin, and eating behavior [67–72].

There is also 6kbp structure [73] that has an average interaction energy of −9.1 kcal/mol. It is a modified human D-amino acid oxidase complexed with benzoate (removed during the docking procedure). The enzyme oxidizes D-amino acids, and in particular *D*-serine, which is connected with the increase in synaptic NMDA receptor activity [74]. Thus, it plays an important role in neurodegenerative diseases [75,76], and schizophrenia is among them [77].

Proteins 2axa, 3vng and 5i6x are presented as examples of structures for which docking did not show good results. The other proteins showed less prominent, but also good results (see supporting information). The calculated energies of protein–ligand interactions are within the range of −4 to −9 kcal/mol.

Synthesized compound **2i** docked into estrogen receptor (4iw8) is shown in Figure 2.

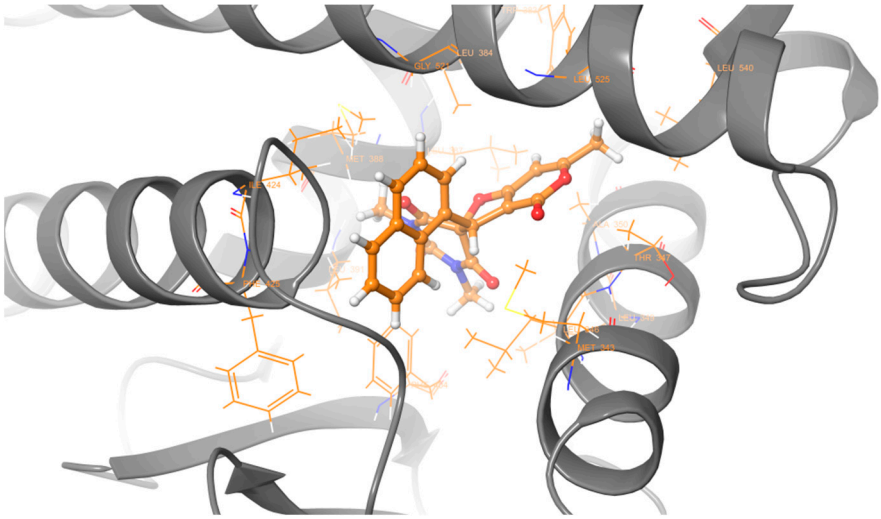

Figure 2. Compound 2i docked into estrogen receptor (4iw8).

4. Conclusions

The new electrocatalytic and efficient assembly of arylaldehydes, *N*,*N*′-dimethylbarbituric acid and 4-hydroxy-6-methyl-2*H*-pyran-2-one in methanol with sodium iodide as mediator in the diaphragmless electrolyzer leads to the formation of the novel spiro[furo[3,2-*c*]pyran-2,5′-pyrimidines] in 73–82% yields.

This earlier unknown electrochemical multicomponent reaction makes it easy to obtain new compounds containing pyrimidine and 2*H*-pyran-2-one cycles, which are promising substances for various biomedical applications.

This electrocatalytic efficient procedure utilizes simple equipment, an undivided cell, an easily available and cheap mediator—sodium iodide—and it is easily carried out and the isolation procedure is very simple.

The automated method was proposed and performed in automated docking procedure. It is distinct from screening by higher accuracy, and it is much more scalable than a classic docking procedure. As it follows from the results, the energies of interaction of many protein–ligands pairs are quite high. 4iw8, 6kbp and 5tlt are the most favourable targets (among 169 proposed targets) from a thermodynamic point of view. Other targets also showed good results. Thus, all synthesized compounds may be prominent for different medical applications, such as breast cancer, neurodegenerative diseases and treatments connected with urinary tract, bones, the cardiovascular system and others.

Supplementary Materials: The following supporting information can be downloaded at: https://www.mdpi.com/article/10.3390/chemistry4020044/s1, ^{1}H and ^{13}C Spectra of synthesized compounds **2a–i** (Figures S1–S18), Single-crystal X-ray Diffraction Data for Compound **2a** (Figure S19, Tables S1–S6). Citation of ref [78,79].

Author Contributions: Conceptualization, M.P.E.; methodology, M.N.E. and F.V.R.; software, F.V.R.; validation, M.N.E., Y.E.R. and A.N.V.; investigation, K.A.K. and I.E.U.; writing—original draft preparation, M.N.E. and K.A.K.; writing—review and editing, Y.E.R.; visualization, F.V.R.; supervision, M.P.E.; project administration, M.N.E. and Y.E.R.; funding acquisition, M.N.E. All authors have read and agreed to the published version of the manuscript.

Funding: This research was funded by RFBR, grant number 19-29-08013.

Institutional Review Board Statement: Not applicable.

Informed Consent Statement: Not applicable.

Data Availability Statement: Not applicable.

Conflicts of Interest: The authors declare no conflict of interest.

Sample Availability: Samples of the compounds **2a-i** are available from the authors.

Appendix A

An archive with the results of molecular docking, as well as scripts for it in the Python programming language, is attached to the article.

References

1. Schneider, P.; Schneider, G. Priviledge structures revisited. *Angew. Chem. Int. Ed.* **2017**, *56*, 7971–7974. [CrossRef] [PubMed]
2. Evans, B.E.; Rittle, K.E.; Bock, M.G.; DiPardo, R.M.; Freidinger, R.M.; Whitter, W.L.; Lundell, G.F.; Veber, D.F.; Anderson, P.S.; Chang, R.S.L.; et al. Methods for drug discovery—Development of potent, selective, orally effective cholecystokinin antagonists. *J. Med. Chem.* **1988**, *31*, 2235–2246. [CrossRef] [PubMed]
3. Zhu, J.; Bienayme, H. (Eds.) *Multicomponent Reactions*; Wiley-VCH Verlag GmbH & Co. KGaA: Weinheim, Germany, 2005. [CrossRef]
4. Ameta, K.L.; Dandia, A.A. (Eds.) *Multicomponent Reactions: Synthesis of Bioactive Heterocycles*; CRS Press: Boca Raton, FL, USA, 2017. [CrossRef]
5. John, S.E.; Gulatia, S.; Shankaraiah, N. Recent advances in multi-component reactions and their mechanistic insights: A triennium review. *Org. Chem. Front.* **2021**, *8*, 4237–4287. [CrossRef]
6. Domling, A.; Wang, W.; Wang, K. Chemistry and biology of multicomponent reactions. *Chem. Rev.* **2012**, *112*, 3083–3135. [CrossRef]
7. Insuasty, D.; Castillo, J.; Becerra, D.; Rojas, H.; Abonia, R. Synthesis of biologically active molecules through multicomponent Reactions. *Molecules* **2020**, *25*, 505. [CrossRef]
8. Younus, H.A.; Al-Rashida, M.; Hameed, A.; Uroos, M.; Salar, U.; Rana, S.; Khan, K.M. Multicomponent reactions (MCR) in medicinal chemistry: A patent review (2010–2020). *Expert Opin. Ther. Pat.* **2021**, *31*, 267–289. [CrossRef]
9. Elinson, M.N.; Ryzhkova, Y.E.; Ryzhkov, F.V. Multicomponent design of chromeno[2,3-*b*]pyridine systems. *Russ. Chem. Rev.* **2021**, *90*, 94–115. [CrossRef]
10. Hammerich, O.; Speiser, B. (Eds.) *Organic Electrochemistry: Revised and Expanded*, 5th ed.; CRC Press: Boca Raton, FL, USA, 2016. [CrossRef]
11. Yan, M.; Kawamata, Y.; Baran, P.S. Synthetic Organic Electrochemistry: Calling All Engineers. *Angew. Chem. Int. Ed.* **2018**, *57*, 4149–4155. [CrossRef] [PubMed]
12. Nikishin, G.I.; Elinson, M.N.; Makhova, I.V. Electrocatalytic haloform reaction: Transformation of methyl ketones into methyl esters. *Angew. Chem. Int. Ed.* **1988**, *27*, 1716–1717. [CrossRef]
13. Wang, X.; She, P.; Zhang, Q. Recent advances on electrochemical methods in fabricating two-dimensional organic-ligand-containing frameworks. *SmartMat* **2021**, *2*, 299–325. [CrossRef]
14. Frankle, R.; Little, D. Redox catalysis in organic electrosynthesis: Basic principles and recent developments. *Chem. Soc. Rev.* **2014**, *43*, 2492–2521. [CrossRef]
15. Ogibin, Y.N.; Elinson, M.N.; Nikishin, G.I. Mediator oxidation systems in organic electrosynthesis. *Russ. Chem. Rev.* **2009**, *78*, 89–140. [CrossRef]
16. Tang, H.-T.; Jia, J.-S.; Pan, Y.-M. Halogen-mediated electrochemical organic synthesis. *Org. Biomol. Chem.* **2020**, *18*, 5315–5333. [CrossRef] [PubMed]
17. Karkas, M.D. Electrochemical strategies for C–H functionalization and C–N bond formation. *Chem. Soc. Rev.* **2018**, *47*, 5786–5865. [CrossRef]
18. Elinson, M.N.; Vereshchagin, A.N.; Ryzhkov, F.V. Catalysis of cascade and multicomponent reactions of carbonyl compounds and C-H acids by electricity. *Chem. Rec.* **2016**, *16*, 1950–1964. [CrossRef]
19. Vereshchagin, A.N.; Elinson, M.N.; Zaimovskaya, T.A.; Nikishin, G.I. Electrocatalytic multicomponent assembling: Stereoselective one-pot synthesis of the substituted 3-azabicyclo[3.1.0]hexane-1-carboxylate system from aldehyde, malononitrile, malonate and methanol. *Tetrahedron* **2008**, *64*, 9766–9770. [CrossRef]
20. Elinson, M.N.; Feducovich, S.K.; Starikova, Z.A.; Vereshchagin, A.N.; Nikishin, G.I. Stereoselective electrocatalytic trans- formation of arylidenemalononitriles and malononitrile into (1*R*,5*S*,6*R*)*-6-aryl-2-amino-4,4-dialkoxy-1,5-dicyano-3-aza- bicyclo[3.1.0]hex-2-enes. *Tetrahedron* **2004**, *60*, 11743–11749. [CrossRef]
21. Elinson, M.N.; Dorofeeva, E.O.; Vereshchagin, A.N.; Nikishin, G.I. Electrochemical synthesis of cyclopropanes. *Russ. Chem. Rev.* **2015**, *84*, 485–497. [CrossRef]

22. Elinson, M.N.; Feducovich, S.K.; Vereshchagin, A.N.; Gorbunov, S.V.; Belyakov, P.A.; Nikishin, G.I. Electrocatalytic multicomponent cyclization of an aldehyde, malononitrile and a malonate into 3-substituted-2,2-dicyanocyclopropane-1,1-dicarboxylate—The first one-pot synthesis of a cyclopropane ring from three different molecules. *Tetrahedron Lett.* **2006**, *47*, 9129–9133. [CrossRef]
23. Elinson, M.N.; Feducovich, S.K.; Bushuev, S.G.; Zakharenkov, A.A.; Pashchenko, D.V.; Nikishin, G.I. Electrochemical transformation of malonate and alkylidenemalonates into 3-substituted cyclopropane-1,1,2,2-tetracarboxylates. *Mendeleev Commun.* **1998**, *8*, 15–17. [CrossRef]
24. Elinson, M.N.; Vereshchagin, A.N.; Ryzkov, F.V. Electrochemical synthesis of heterocycles via cascade reactions. *Curr. Org. Chem.* **2017**, *21*, 1427–1439. [CrossRef]
25. Taylor, A.P.; Robinson, R.P.; Fobian, Y.M.; Blamore, D.C.; Jones, L.H.; Fadeyi, O. Modern advances in heterocyclic chemistry in drug discovery. *Org. Biomol. Com.* **2016**, *2016*, 6611–6637. [CrossRef]
26. Yet, L. *Privileged Structures in Drug Discovery: Medicinal Chemistry and Synthesis*; John Wiley & Sons, Inc.: Hoboken, NJ, USA, 2018. [CrossRef]
27. Katsamakas, S.; Papadopoulos, A.G.; Kouskoura, M.G.; Markopoulou, C.K. Examining barbiturate scaffold for the synthesis of new agents with biological interest. *Future Med. Chem.* **2019**, *11*, 2063–2079. [CrossRef] [PubMed]
28. Brunton, L.L.; Lazo, J.S.; Parker, K.L.; Buxton, I.; Blumenthal, D. *Goodman and Gilman's: The Pharmacological Basis of Therapeutics*, 11th ed.; The McGraw-Hill Companies, Inc.: New York, NY, USA, 2006. [CrossRef]
29. Uhlmann, C.; Froscher, W. Low Risk of Development of Substance Dependence for Barbiturates and Clobazam Prescribed as Antiepileptic Drugs: Results from a Questionnaire Study. *CNS Neurosci. Ther.* **2009**, *15*, 24–31. [CrossRef] [PubMed]
30. Johns, M.W. Sleep and Hypnotic Dugs. *Drugs* **1975**, *9*, 448–478. [CrossRef] [PubMed]
31. Grams, F.; Brandstetter, H.; D'Alo, S.; Geppert, D.; Krell, Y.W.; Leinert, H.; Livi, V.; Menta, E.; Oliva, A.; Zimmermann, G. Pyrimidine-2,4,6-triones: A new effective and selective class of matrix metalloproteinase inhibitors. *Biol. Chem.* **2001**, *382*, 1277–1285. [CrossRef] [PubMed]
32. Gruber, P.; Rechfeld, F.; Kirchmair, J.; Hauser, N.; Boehler, M.; Garczarczyk, D.; Langer, T.; Hofmann, J. Barbituric acid derivative BAS 02104951 inhibits PKCε, PKCη, KCε/RACK2 interaction, Elk-1 phosphorylation in HeLa and PKCε and η translocation in PC3 cells following TPA-induction. *J. Biochem.* **2011**, *149*, 331–336. [CrossRef]
33. Prasad, J.V.N.V.; Pavlovsky, A.; Para, K.S.; Ellsworth, E.L.; Tummino, P.J.; Nouhan, C.; Ferguson, D. Nonpeptidic HIV protease inhibitors: 3-(*S*-benzyl substituted)-4-hydroxy-6-(phenyl substituted)-2*H*-pyran-2-one with an inverse mode of binding. *Bioorg. Med. Chem. Lett.* **1996**, *6*, 1133–1138. [CrossRef]
34. Lan, Q.-Y.; Liu, Q.-L.; Cai, J.; Liu, A.-W. 3-Cinnamoyl-4-hydroxy-6-methyl-2*H*-pyran-2-one (CHP) inhibits human ovarian cell proliferation by inducing apoptosis. *Int. J. Clin. Exp. Pathol.* **2015**, *8*, 155–163. Available online: https://e-century.us/files/ijcep/8/1/ijcep0003810.pdf (accessed on 7 April 2022).
35. Yin, P.-H.; Liu, X.; Qiu, Y.-Y.; Cai, J.-F.; Qin, J.-M.; Zhu, H.-R.; Li, Q. Anti-tumor activity and apoptosis-regulation mechanisms of bufalin in various cancers: New hope for cancer patients. *Asian Pac. J. Cancer Prev.* **2012**, *13*, 5329–5343. [CrossRef]
36. Tsuchiya, K.; Kobayashi, S.; Nishikiori, T.; Nakagawa, T.; Tatsuta, K. NK10958P, a novel plant growth regulator produced by *Streptomyces* sp. *J. Antibiot.* **1997**, *50*, 259–260. [CrossRef]
37. Kondoh, M.; Usui, T.; Kobayashi, S.; Tsuchiya, K.; Nishikawa, K.; Nishikiori, T.; Mayumi, T.; Osada, H. Cell cycle arrest and antitumor activity of pironetin and its derivatives. *Cancer Lett.* **1998**, *126*, 29–32. [CrossRef]
38. Turner, S.R.; Strohbach, J.W.; Tommasi, R.A.; Aristoff, P.A.; Johnson, P.D.; Shulnick, H.I.; Dolak, L.A.; Seest, E.P.; Tomich, P.K.; Bohanon, M.J.; et al. Tipranavir (PNU-140690): A potent, orally bioavailable nonpeptidic HIV protease inhibitor of the 5,6-dihydro-4-hydroxy-2-pyrone sulfonamide class. *J. Med. Chem.* **1998**, *41*, 3467–3476. [CrossRef] [PubMed]
39. Zheng, Y.; Tice, C.M.; Singh, S.B. The use of spirocyclic scaffolds in drug discovery. *Bioorg. Med. Chem. Lett.* **2014**, *24*, 3673–3682. [CrossRef]
40. Zheng, Y.; Tice, C.M. The utilization of spirocyclic scaffolds in novel drug discovery. *Expert Opin. Drug Discov.* **2016**, *11*, 831–834. [CrossRef] [PubMed]
41. Müller, G.; Berkenbosch, T.; Benningshof, J.C.J.; Stumpfe, D.; Bajorath, J. Charting biologically relevant spirocyclic compound space. *Chem. Eur. J.* **2017**, *23*, 703–710. [CrossRef] [PubMed]
42. Hiesinger, K.; Dar'in, D.; Proschak, E.; Krasavin, M. Spirocyclic Scaffolds in Medicinal Chemistry. *J. Med. Chem.* **2021**, *64*, 150–183. [CrossRef] [PubMed]
43. Galati, E.M.; Monforte, M.T.; Miceli, N.; Ranerill, E. Anticonvulsant and sedative effects of some 5-substituted bromopyrazolinic-spirobarbiturates. *Farmaco* **2001**, *56*, 459–461. [CrossRef]
44. Kim, S.-H.; Pudzianowski, A.T.; Leavitt, K.J.; Barbosa, J.; McDonnell, P.A.; Metzler, W.J.; Rankin, B.M.; Liu, R.; Vaccaro, W.; Pitts, W. Structure-based design of potent and selective inhibitors of collagenase-3 (MMP-13). *Bioorg. Med. Chem. Lett.* **2005**, *15*, 1101–1106. [CrossRef]
45. Fraser, W.; Suckling, C.J.; Wood, H.C.S. Latent inhibitors. Part 7. Inhibition of dihydro-orotate dehydrogenase by spirocyclopropanobarbiturates. *J. Chem. Soc. Perkin Trans. 1* **1990**, *1*, 3137–3144. [CrossRef]
46. Duan, J.; Jiang, B.; Chen, L.; Lu, Z.; Barbosa, J.; Pitts, W.J. Barbituric Acid Derivatives as Inhibitors of the TNF-Alpha Convertingenzyme (TACE) and/or Matrix Metalloproteinases. U.S. Patent WO2003053941, 3 July 2003. Available online: https://patentscope.wipo.int/search/en/detail.jsf?docId=WO2003053941 (accessed on 7 April 2022).

47. Elinson, M.N.; Dorofeeva, E.O.; Vereshchagin, A.N.; Nasybullin, R.F.; Egorov, M.P. Electrocatalytic stereoselective transformation of aldehydes and two molecules of pyrazolin-5-one into (*R**,*R**)-bis(spiro-2,4-dihydro-3*H*-pyrazol-3-one)cyclopro- panes. *Catal. Sci. Technol.* **2015**, *5*, 2384–2387. [CrossRef]
48. Vereshchagin, A.N.; Elinson, M.N.; Egorov, M.P. The first electrocatalytic stereoselective multicomponent synthesis of cyclopropanecarboxylic acid derivatives. *RCS Adv.* **2015**, *5*, 98522–98526. [CrossRef]
49. Vereshchagin, A.N.; Elinson, M.N.; Dorofeeva, E.O.; Stepanov, N.O.; Zaimovskaya, T.A.; Nikishin, G.I. Electrocatalytic and chemical methods in MHIRC reactions: The first example of the multicomponent assembly of medicinally relevant spirocyclopropylbarbiturates from three different molecules. *Tetrahedron* **2013**, *69*, 1945–1952. [CrossRef]
50. Vereshchagin, A.N.; Elinson, M.N.; Dorofeeva, E.O.; Zaimovskaya, T.A.; Stepanov, N.O.; Gorbunov, S.V.; Belyakov, P.A.; Nikishin, G.I. Electrocatalytic and chemical assembling of *N*,*N*′-dialkylbarbituric acids and aldehydes: Efficient cascade approach to the spiro[furo[2,3-*d*]pyrimidine-6,5′-pyrimidine]-2,2′,4,4′,6′-(1′*H*,3*H*,3′*H*)-pentone framework. *Tetrahedron* **2012**, *68*, 1198–1206. [CrossRef]
51. Elinson, M.N.; Vereshchagin, A.N.; Stepanov, N.O.; Belyakov, P.A.; Nikishin, G.I. Cascade assembly of *N*,*N*′-dialkylbarbituric acids and aldehydes: A simple and efficient one-pot approach to the substituted 1,5-dihydro-2*H*,2′*H*-spiro(furo[2,3-*d*]pyrimidine-6,5′-pyrimidine)-2,2′,4,4′,6′(1′*H*,3*H*,3′*H*)-pentone framework. *Tetrahedron Lett.* **2010**, *51*, 6598–6601. [CrossRef]
52. *Bruker APEX-III*; Bruker AXS Inc.: Madison, WI, USA, 2019.
53. Krause, A.L.; Herbst-Irmer, R.; Sheldrick, G.M.; Stalke, D. Comparison of silver and molybdenum microfocus X-ray sources for single-crystal structure determination. *J. Appl. Crystallogr.* **2015**, *48*, 3–10. [CrossRef] [PubMed]
54. Sheldrick, G.M. *SHELXT*—Integrated space-group crystal-structure determination. *Acta Crystallogr.* **2015**, *A71*, 3–8. [CrossRef]
55. Sheldrick, G.M. Crystal structure refinement with *SHELXL*. *Acta Crystallogr.* **2015**, *C71*, 3–8. [CrossRef]
56. Dorofeeva, E.O.; Elinson, M.N.; Vereshchagin, A.N.; Stepanov, N.O.; Bushmarinov, I.S.; Belyakov, P.A.; Sokolova, O.O.; Nikishin, G.I. Electrocatalysis in MIRC reaction strategy: Facile stereoselective approach to medicinally relevant spirocyclopropylbarbiturates from barbituric acids and activated olefins. *RCS Adv.* **2012**, *2*, 4444–4452. [CrossRef]
57. Elinson, M.N.; Fedukovich, S.K.; Vereshchagin, A.N.; Dorofeev, A.S.; Dmitriev, D.V.; Nikishin, G.I. Electrocatalytic transformation of malononitrile and cycloalkylidenemalononitriles into spirobicyclic and spirotricyclic compounds containing 1,1,2,2-tetracyanocyclopropane fragment. *Russ. Chem. Bull.* **2003**, *52*, 2235–2240. [CrossRef]
58. Elinson, M.N.; Lizunova, T.L.; Dekaprilevich, M.O.; Struchkov, Y.T.; Nikishin, G.I. Electrochemical cyclotrimerization of cyanoacetic ester into *trans*-1,2,3-tricyanocyclopropane-1,2,3-tricarboxylate. *Mendeleev Commun.* **1993**, *3*, 192–193. [CrossRef]
59. *Flare, Version 5.0.0*; Cresset: Litlington, UK, 2021. Available online: http://www.cresset-group.com/flare/ (accessed on 7 April 2022).
60. Cheeseright, T.; Mackey, M.; Rose, S.; Vinter, A. Molecular Field Extrema as Descriptors of Biological Activity: Definition and Validation. *J. Chem. Inf. Model.* **2006**, *46*, 665–676. [CrossRef] [PubMed]
61. Bauer, M.R.; Mackey, M.D. Electrostatic Complementarity as a Fast and Effective Tool to Optimize Binding and Selectivity of Protein–Ligand Complexes. *J. Med. Chem.* **2019**, *62*, 3036–3050. [CrossRef] [PubMed]
62. Kuhn, M.; Firth-Clark, S.; Tosco, P.; Mey, A.S.J.S.; Mackey, M.; Michel, J. Assessment of Binding Affinity via Alchemical Free-Energy Calculations. *J. Chem. Inf. Model.* **2020**, *60*, 3120–3130. [CrossRef] [PubMed]
63. *Lead Finder, Version 2104 Build 1*; BioMolTech: Toronto, ON, Canada, 2021. Available online: http://www.cresset-group.com/lead-finder/ (accessed on 7 April 2022).
64. Battles, M.; Langedijk, J.; Furmanova-Hollenstein, P.; Chaiwatpongsakorn, S.; Costello, H.M.; Kwanten, L.; Vranckx, L.; Vink, P.; Jaensch, S.; Jonckers, T.H.M.; et al. Molecular mechanism of respiratory syncytial virus fusion inhibitors. *Nat. Chem. Biol.* **2016**, *12*, 87–93. [CrossRef] [PubMed]
65. Nwachukwu, J.C.; Srinivasan, S.; Bruno, N.E.; Nowak, J.; Wright, N.J.; Minutolo, F.; Rangarajan, E.S.; Izard, T.; Yao, X.-Q.; Grant, B.; et al. Systems Structural Biology Analysis of Ligand Effects on ERα Predicts Cellular Response to Environmental Estrogens and Anti-hormone Therapies. *Cell Chem. Biol.* **2017**, *24*, 35–45. [CrossRef] [PubMed]
66. Li, F.; Dou, J.; Wei, L.; Li, S.; Liu, J. The selective estrogen receptor modulators in breast cancer prevention. *Cancer Chemother. Pharmacol.* **2016**, *77*, 895–903. [CrossRef] [PubMed]
67. Bondesson, M.; Hao, R.; Lin, C.-Y.; Williams, C.; Gustafsson, J.-Å. Estrogen receptor signaling during vertebrate development. *Biochim. Biophys. Acta* **2015**, *1849*, 142–151. [CrossRef]
68. dos Santos, R.L.; da Silva, F.B.; Ribeiro, R.F.; Stefanon, I. Sex hormones in the cardiovascular system. *Horm. Mol. Biol. Clin. Investig.* **2014**, *18*, 89–103. [CrossRef]
69. Arnal, J.-F.; Lenfant, F.; Metivier, R.; Flouriot, G.; Henrion, D.; Adlanmerini, M.; Fontaine, C.; Gourdy, P.; Chambon, P.; Katzenellenbogen, B.; et al. Membrane and Nuclear Estrogen Receptor Alpha Actions: From Tissue Specificity to Medical Implications. *Physiol. Rev.* **2017**, *97*, 1045–1087. [CrossRef]
70. Hirschberg, A.L. Sex hormones, appetite and eating behaviour in women. *Maturitas* **2012**, *71*, 248–256. [CrossRef] [PubMed]
71. Simpson, E.R. Sources of estrogen and their importance. *J. Steroid Biochem. Mol.* **2003**, *86*, 225–230. [CrossRef]
72. Turgeon, J.L.; McDonnell, D.P.; Martin, K.A.; Wise, P.M. Hormone therapy: Physiological complexity belies therapeutic simplicity. *Science* **2004**, *304*, 1269–1273. [CrossRef] [PubMed]
73. Rachadech, W.; Kato, Y.; El-Magd, R.M.A.; Shishido, Y.; Kim, S.H.; Sogabe, H.; Maita, N.; Yorita, K.; Fukui, K. P219L substitution in human D-amino acid oxidase impacts the ligand binding and catalytic efficiency. *J. Biochem.* **2020**, *168*, 557–567. [CrossRef]

74. Pollegioni, L.; Piubelli, L.; Sacchi, S.; Pilone, M.S.; Molla, G. Physiological functions of D-amino acid oxidases: From yeast to humans. *Cell. Mol. Life Sci.* **2007**, *64*, 1373–1394. [CrossRef]
75. Madeira, C.; Freita, M.E.; Vargas-Lopes, C.; Wolosker, H.; Panizzutti, R. Increased brain d-amino acid oxidase (DAAO) activity in schizophrenia. *Schizophr. Res.* **2008**, *101*, 76–83. [CrossRef]
76. Boks, M.P.M.; Rietkerk, T.; van de Beek, M.H.; Sommer, I.E.; de Koning, T.J.; Kahn, R.S. Reviewing the role of the genes G72 and DAAO in glutamate neurotransmission in schizophrenia. *Eur. Neuropsychopharmacol.* **2007**, *17*, 567–572. [CrossRef]
77. Verrall, L.; Burnet, P.W.J.; Betts, J.F.; Harrison, P.J. The neurobiology of D-amino acid oxidase and its involvement in schizophrenia. *Mol. Psychiatry* **2010**, *15*, 122–137. [CrossRef]
78. Dolomanov, O.V.; Bourhis, L.J.; Gildea, R.J.; Howard, J.A.K.; Puschmann, H. OLEX2: A complete structure solution, refinement and analysis program. *J. Appl. Cryst.* **2009**, *42*, 339–341. [CrossRef]
79. Sheldrick, G.M. A short history of SHELX. *Acta Cryst.* **2008**, *A64*, 112–122. [CrossRef]